
Mitigating Hidden Confounding by Progressive Confounder Imputation via Large Language Models

Hao Yang¹ Haoxuan Li² Luyu Chen¹ Haoxiang Wang³
 Xu Chen^{1*} Mingming Gong^{4*}

¹Gaoling School of Artificial Intelligence, Renmin University of China

²Center for Data Science, Peking University

³School of Mathematical Sciences, Peking University

⁴Department of Machine Learning, Mohamed bin Zayed University of Artificial Intelligence
 hao.yang@ruc.edu.cn, hxli@stu.pku.edu.cn, luyu.chen@ruc.edu.cn,
 whxwhx@pku.edu.cn, xu.chen@ruc.edu.cn, mingming.gong@unimelb.edu.au

Abstract

Hidden confounding remains a central challenge in estimating treatment effects from observational data, as unobserved variables can lead to biased causal estimates. While recent work has explored the use of large language models (LLMs) for causal inference, most approaches still rely on the unconfoundedness assumption. In this paper, we make the first attempt to mitigate hidden confounding using LLMs. We propose ProCI (Progressive Confounder Imputation), a framework that elicits the semantic and world knowledge of LLMs to iteratively generate, impute, and validate hidden confounders. ProCI leverages two key capabilities of LLMs: their strong semantic reasoning ability, which enables the discovery of plausible confounders from both structured and unstructured inputs, and their embedded world knowledge, which supports counterfactual reasoning under latent confounding. To improve robustness, ProCI adopts a distributional reasoning strategy instead of direct value imputation to prevent the collapsed outputs. Extensive experiments demonstrate that ProCI uncovers meaningful confounders and significantly improves treatment effect estimation across various datasets and LLMs.

1 Introduction

Estimating treatment effects from observational data is a central problem in causal inference, with widespread applications in healthcare [40, 16], social sciences [14], and economics [49, 47]. Different from Randomized Controlled Trials (RCTs), the non-random treatment assignments between treatment and control groups in observational studies can lead to imbalanced confounders between groups, which has been recognized as a key contributor to non-causal indirect associations [37]. The bias caused by imbalanced confounders is referred to as confounding bias [46, 51].

To estimate treatment effects in an unbiased manner from observational data, recent advances have focused on representation-based methods that aim to balance latent distributions between treatment and control groups [46, 51, 6, 56]. More recently, with the emergence of large language models (LLMs) demonstrating remarkable capabilities in reasoning and knowledge understanding, a plenty of work has begun to explore their potential in treatment effect estimation [35, 22, 26, 18, 23]. For example, [26] prompts LLMs using chain-of-thought reasoning to generate natural language rationales that support causal conclusions, while [23] leverages LLMs to encode high-dimensional text treatments for treatment effect estimation while mitigating confounding.

*Corresponding authors.

However, existing methods including those based on LLMs, mostly rely on the *unconfoundedness assumption* [37], which posits that all confounders affecting both treatment and outcome are observed. This assumption is often unrealistic in real-world settings, where important factors may be unobserved or entirely unrecorded [5]. For example, in healthcare, treatment decisions may be influenced not only by observed clinical features such as test results or age, but also by unobserved factors like socioeconomic status, which can act as confounders if omitted. To address hidden confounding issue, prior work has explored three main directions. Sensitivity analysis aims to quantify the impact of hidden confounding by deriving bounds on treatment effects [43, 42], but typically relies on fixed and untestable assumptions about the confounding mechanism [12, 50]. Auxiliary variable methods, including instrumental variables and front-door adjustment, use external information or intermediate pathways to recover unbiased estimates [30, 13, 45], but depend on strong structural assumptions that are rarely verifiable [24, 53, 7]. RCT integration methods combine randomized and observational data to correct for hidden confounding bias [27, 19, 55], but the high cost and limited availability of RCTs often restrict their practical utility.

To fill this gap, we make the first attempt to leverage LLMs to mitigate hidden confounding in treatment effect estimation. Compared to traditional methods, LLMs offers two key advantages. First, LLMs possess strong semantic reasoning capabilities that allow them to interpret both structured covariates and unstructured textual descriptions, enabling the discovery of plausible confounders that are not explicitly recorded in the data. Second, LLMs embed extensive world knowledge learned from large-scale corpora, which implicitly captures a wide range of latent confounders, allowing them to support counterfactual reasoning even under hidden confounding.

To elicit these capabilities in practice, we propose **ProCI** (Progressive Confounder Imputation), a novel framework that leverages LLMs to iteratively uncover and adjust for hidden confounders. ProCI alternates between two phases: (1) *confounder imputation*, where the LLM is prompted to generate a plausible missing confounder based on the semantics of the observed variables, and to impute its concrete values; and (2) *unconfoundedness validation*, which builds on the LLM’s counterfactual reasoning ability—by prompting the LLM to impute missing potential outcomes, we empirically test whether the generated confounders restore conditional independence between treatment and outcomes. Rather than directly predicting values, which we find empirically leads to collapsed or inconsistent outputs, ProCI adopts a distributional reasoning strategy: it first elicits from the LLM the most plausible distribution type based on its world knowledge, and then infers distribution parameters to generate diverse, realistic samples. This progressive process continues until the generated confounders pass the independence test, indicating that key sources of hidden confounding have been mitigated. By incorporating LLMs into the treatment effect estimation pipeline, ProCI provides a flexible and scalable solution for mitigating hidden confounding in observational studies. Our contributions can be summarized as follows:

- To the best of our knowledge, this is the first work that leverages LLMs to mitigate hidden confounding in treatment effect estimation. This is enabled by eliciting both the semantic signals in observational data and the implicit confounding knowledge embedded in LLMs.
- We propose ProCI, a progressive framework that elicits LLMs to generate and impute plausible confounders by jointly leveraging textual descriptions and structured covariates. The sufficiency of the generated confounders is validated through LLM-based counterfactual prediction and an empirical test of conditional independence.
- Extensive experiments across diverse datasets and multiple LLM architectures demonstrate the effectiveness and generality of our approach, showing improved performance in uncovering hidden confounders and estimating treatment effects.

2 Preliminaries

2.1 Problem Setup

We consider the standard setup in binary treatment effect estimation². Let $T \in \{0, 1\}$ denote a binary treatment assignment, where $T = 1$ indicates receiving the treatment and $T = 0$ denotes the control group. Let $Y \in \mathbb{R}$ be the observed outcome, and $X \in \mathcal{X}$ be the observed covariates. The

²While we focus on the binary treatment setting for clarity, the proposed method of this paper can be directly extended to other scenarios, such as multi-valued or continuous treatments.

observational dataset consists of i.i.d. samples $\{(x_i, t_i, y_i)\}_{i=1}^n \sim \mathcal{D}$. Under the potential outcomes framework [44], each unit is associated with two potential outcomes: Y^1 and Y^0 , representing the outcomes the unit would receive under treatment and control, respectively. In practice, only one factual outcome Y is observed for each unit, depending on the assigned treatment. The individual-level treatment effect is defined as:

$$\tau(x) = \mathbb{E}[Y^1 - Y^0 \mid X = x], \quad (1)$$

which is commonly referred to as the *Conditional Average Treatment Effect* (CATE) [2]. It quantifies the expected difference in potential outcomes for a given covariate profile x , and serves as the primary estimand of interest in individual-level treatment effect estimation.

2.2 Identifiability Assumptions

CATE estimation from observational data requires a set of identifiability assumptions [37]. These include the consistency assumption, where the observed outcome corresponds to the potential outcome under the treatment received and there is no interference between units, and the positivity assumption, which ensures that for all covariate values, the probability of receiving any treatment is strictly positive. This paper focuses on unconfoundedness assumption, which we formally define as follows:

Assumption 1 (Unconfoundedness). *The treatment assignment is independent of the potential outcomes, conditional on the observed covariates, i.e.,*

$$(Y^1, Y^0) \perp\!\!\!\perp T \mid X. \quad (2)$$

When these assumptions hold, the CATE function in Eq. (1) becomes identifiable and is expressed as:

$$\tau(x) = \mathbb{E}[Y \mid T = 1, X = x] - \mathbb{E}[Y \mid T = 0, X = x], \quad (3)$$

which can be directly estimated from a finite observational dataset \mathcal{D} by learning an estimator $\hat{\tau}(x)$, e.g., using CFRNet or TARNet [46], that approximates the true CATE function $\tau(x)$.

Hidden Confounding Challenge. However, in practice, the assumption of unconfoundedness can be easily violated due to limited context [25], where observed covariates X do not capture all relevant confounders that jointly affect treatment and outcome. In particular, treatment assignment may depend on hidden variables U that also influence the outcome Y . In such cases, the conditional independence assumption $(Y^1, Y^0) \perp\!\!\!\perp T \mid X$ is no longer valid, and is instead replaced by $(Y^1, Y^0) \not\perp\!\!\!\perp T \mid X$, but possibly $(Y^1, Y^0) \perp\!\!\!\perp T \mid (X, U)$ if U were additionally observed. This hidden confounding results in a systematic estimation bias: the learned estimator $\hat{\tau}(x)$, which assumes unconfoundedness given X , is biased with respect to the true CATE $\tau(x)$.

3 The Proposed ProCI Framework

3.1 Motivation

As aforementioned, hidden confounding is a fundamental challenge in observational study, as it can severely bias treatment effect estimates. Although a range of methods have been proposed to mitigate this issue, including auxiliary variables, sensitivity analysis, and data from RCTs, these approaches either rely on untestable assumptions or are prohibitively expensive to apply in practice [5].

Motivated by these limitations, we propose a new paradigm for addressing hidden confounding through LLMs. Leveraging their unique capabilities, this paper makes the first attempt to directly mitigate hidden confounding using LLMs, based on two key advantages:

- **Advantage 1: Semantic Utilization Beyond Tabular Data.** Traditional methods typically rely on structured tabular data and predefined variable sets, making it difficult to discover missing confounders that are not explicitly recorded. In contrast, as shown in Figure 1 (A1-1) and (A1-2), LLMs can generate meaningful confounder candidates by interpreting the semantic relationships among treatment, outcome, and observed covariates. This demonstrates the LLM’s ability to reason about plausible latent variables using domain-level priors encoded in language. Subsequently, by leveraging the existing tabular data, the LLM can perform unit-level confounder imputation based on its contextual inference capabilities to complete missing data.

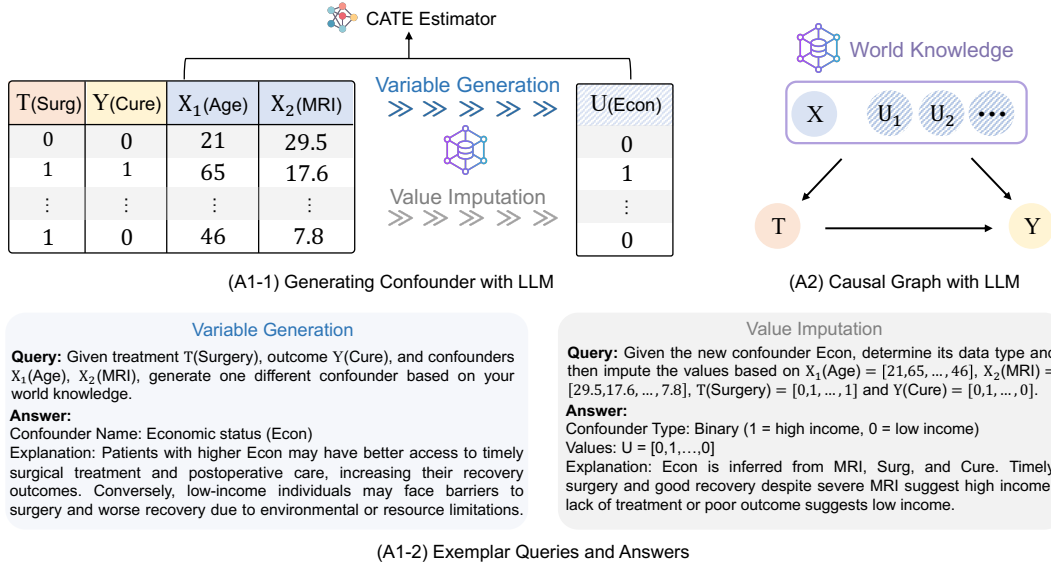


Figure 1: Illustration of how LLMs help mitigate hidden confounding. **(A1-1)** The LLM takes structured data (treatment T , outcome Y , covariates X) to generate a missing confounder and impute its individual-level values for CATE estimation. **(A1-2)** Example prompts and responses show how LLMs leverage semantic and world knowledge in variable generation and value imputation. **(A2)** From a causal perspective, LLMs embed latent confounders within their world knowledge, enabling counterfactual reasoning without requiring explicit access to them.

• **Advantage 2: Implicit Confounding Awareness via World Knowledge.** Beyond explicit confounder generation, LLMs inherently encode rich world knowledge that implicitly captures causal dependencies and latent confounding factors. As illustrated in Figure 1 (A2), this embedded knowledge allows LLMs to approximate the influence of hidden variables and thus support counterfactual reasoning without requiring direct access to all confounders. Such implicit awareness makes LLMs particularly suited for scenarios where collecting complete causal information is impractical, offering a scalable and assumption-light alternative to traditional approaches. This advantage becomes increasingly valuable as the complexity and dimensionality of real-world data continue to grow.

3.2 Overview of the ProCI Framework

To elicit the above capabilities of LLMs for practical use, we propose ProCI, a framework for mitigating hidden confounding in observational data. As illustrated in Figure 2, ProCI consists of two iterative phases: *confounder imputation* and *unconfoundedness validation*.

Phase 1: Confounder Imputation. Given the observed dataset $\{X^{(0)}, T, Y\}$, where $X^{(0)}$ contains structured covariates, ProCI first prompts the LLM to generate a plausible confounder variable \hat{U} based on the semantic relationships among $X^{(k)}$, T , and Y . The LLM also provides a textual explanation for the generated variable. Next, the framework imputes instance-level values for \hat{U} by determining its distribution type and estimating the corresponding parameters using LLM-guided reasoning. The imputed confounder is then appended to the dataset to form $X^{(k+1)}$.

Phase 2: Unconfoundedness Validation. To assess whether the generated confounder \hat{U} captures sufficient hidden bias, ProCI performs an imputation-based empirical unconfoundedness test. Specifically, since the LLM encodes hidden confounding information within its world knowledge representation, ProCI leverages this capability to impute the counterfactual outcomes \hat{Y}^0 and \hat{Y}^1 . Then, a kernel-based conditional independence test (KCIT) is applied to check whether $(\hat{Y}^0, \hat{Y}^1) \perp\!\!\!\perp T \mid X^{(k+1)}$. If the test fails, ProCI returns to Phase 1 to generate an additional confounder. If the test passes, the framework proceeds to estimate the CATE using any standard estimator, such as TARNet.

By progressively generating and validating confounders, ProCI adaptively constructs a sufficient adjustment set without requiring access to ground-truth confounding variables, enabling more reliable treatment effect estimation in the presence of hidden confounding bias.

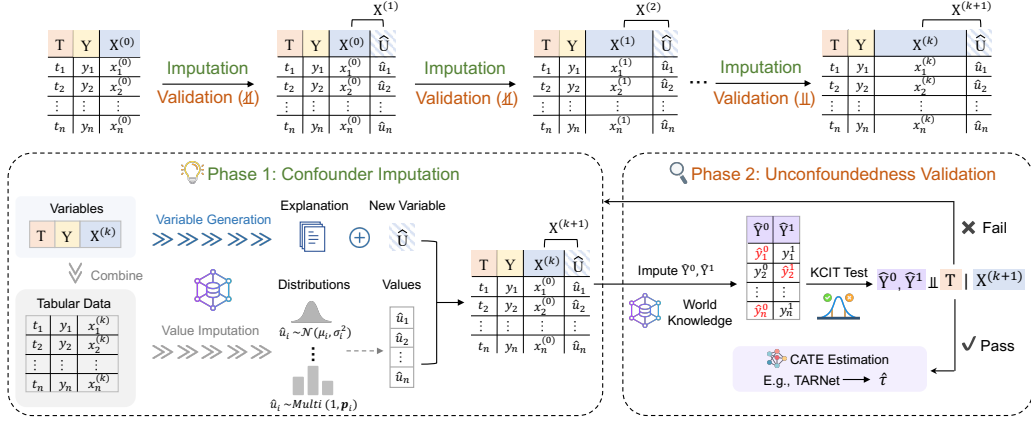


Figure 2: Overview of the ProCI framework. ProCI alternates between two phases: (1) Confounder Imputation, where the LLM generates a new confounder and imputes its instance-level values based on current variables. (2) Unconfoundedness Validation, where counterfactual outcomes are imputed and a KCIT is applied to assess whether unconfoundedness holds. The process repeats until the test passes, after which any standard estimator can be used for final CATE estimation.

3.3 Confounder Imputation via Prompting LLMs

In this section, we propose to prompt LLMs to generate hidden confounders that are semantically grounded and causally relevant. Imputing a confounder involves two key steps: (1) generating a variable with a meaningful textual description, and (2) imputing its concrete values for each individual in the dataset. We describe these steps in detail below.

Variable Generation. Given a dataset \mathcal{D}_{obs} consisting of observed variables $\{X, T, Y\}$, where X denotes covariates, T the treatment, and Y the outcome, we first design a prompt function \mathcal{P}_{var} to convert the textual descriptions of these variables into a natural language query. We then use this prompt to query the LLM for a candidate confounder variable \hat{U} that is semantically associated with both T and Y , while being orthogonal to X :

$$\hat{U}, \hat{U}_{\text{exp}} = \text{LLM}(\mathcal{P}_{\text{var}}(X, T, Y)), \quad (4)$$

where \hat{U} is the name or description of the generated confounder, and \hat{U}_{exp} is the accompanying natural language explanation provided by the LLM. This explanation enhances the interpretability of the generation process and can serve as supporting evidence for the semantic plausibility of \hat{U} .

Value Imputation. After generating the confounder variable \hat{U} , we next impute its values for each individual to obtain an augmented dataset $\hat{\mathcal{D}}_{\text{obs}} = \{x_i, t_i, y_i, \hat{u}_i\}_{i=1}^N$. Direct value imputation, i.e., prompting the LLM to generate \hat{u}_i for each individual via a single-pass query, tends to produce collapsed outputs where many individuals receive similar or identical values. To address this issue, we decompose value imputation into distribution identification and parameter inference as below.

Distribution Identification. Intuitively, by leveraging its embedded commonsense and world knowledge, the LLM can reliably identify the distribution type of a variable, for example, inferring that height follows a normal distribution, while birth month is approximately uniform in a community. Therefore, for the generated variable \hat{U} , we can confidently prompt the LLM to identify a reasonable distribution type $\mathcal{F} \in \mathbb{F} = \{\mathcal{F}_z\}_{z=1}^Z$:

$$\mathcal{F} \sim \text{LLM}(\mathcal{P}_{\text{dist}}(X, T, Y, \hat{U})) \mid \mathcal{F} \in \mathbb{F}. \quad (5)$$

In practice, the candidate distribution types \mathbb{F} include, but are not limited to, Gaussian, Bernoulli, and categorical distributions.

Parameter Inference. Once the distribution family \mathcal{F} is selected, we prompt the LLM to infer individual-specific distribution parameters θ_i based on each individual's observed features. For example, $\theta_i = (\mu_i, \sigma_i)$ if \mathcal{F} is a normal distribution. We then sample the imputed value \hat{u}_i from the corresponding personalized distribution:

$$\theta_i = \text{LLM}(\mathcal{P}_{\text{param}}(x_i, t_i, y_i)), \quad \hat{u}_i \sim \mathcal{F}(\theta_i). \quad (6)$$

Compared to direct value imputation, this decomposition strategy helps reduce uncertainty and mitigates the collapse effect often observed in LLM outputs, thereby providing a more robust and controllable way for confounder value generation.

3.4 Imputation-based Empirical Unconfoundedness Test

While LLMs can help to impute the confounder, it is still challenging to test the validity of the generated confounder. Intuitively, a crucial criterion is the unconfoundedness assumption (Assumption 1): once conditioned on both the observed and generated confounders X and \hat{U} , the treatment variable T should be independent of the potential outcomes Y^0 and Y^1 . However, in observational datasets, we can only observe one of these two potential outcomes for each individual, making empirical testing of the unconfoundedness assumption seemingly infeasible.

To bridge this gap, we propose using LLMs to impute the missing outcomes Y^0 and Y^1 as follows:

$$\hat{y}_i^{1-t_i} = \text{LLM}(\mathcal{P}_{\text{out}}(x_i, u_i, t_i, y_i)). \quad (7)$$

Then, we construct the variables \hat{Y}^0 and \hat{Y}^1 , where for each individual i :

$$\hat{y}_i^0 = (1 - t_i) \cdot y_i + t_i \cdot \hat{y}_i^{1-t_i}, \quad \hat{y}_i^1 = t_i \cdot y_i + (1 - t_i) \cdot \hat{y}_i^{1-t_i}. \quad (8)$$

Rationality Analysis. Since LLMs embed extensive world knowledge that potentially covers all relevant hidden confounders U^* , they can be viewed as approximately unbiased counterfactual estimators under the unconfoundedness assumption. That is, when conditioned on the full context accessible to the LLM—including both structured and unstructured information—the potential outcomes (Y^0, Y^1) become independent of the treatment T . Formally, we posit that the LLM implicitly conditions on a latent variable U^* such that $(Y^0, Y^1) \perp\!\!\!\perp T \mid X, U^*$, where U^* denotes a sufficient set of hidden confounders encoded in the LLM’s prior knowledge. This supports the use of LLMs for counterfactual prediction.

After obtaining the imputed outcomes \hat{Y}^0 and \hat{Y}^1 , we can statistically test the unconfoundedness assumption using a non-parametric independence test. Specifically, we adopt the Kernel-based Conditional Independence Test (KCIT), which is well-suited for high-dimensional conditioning sets [39]. KCIT evaluates whether the treatment T is conditionally independent of the imputed outcomes (\hat{Y}^0, \hat{Y}^1) given the observed and generated confounders X and \hat{U} :

$$\mathbb{I}(\text{KCIT}((\hat{Y}^0, \hat{Y}^1), T \mid X, \hat{U}) > \alpha) = 1, \quad (9)$$

where $\text{KCIT}(\cdot)$ returns a p -value, and α is a pre-defined significance level. The indicator function $\mathbb{I}(\cdot)$ outputs 1 if the null hypothesis of conditional independence is not rejected, and 0 otherwise.

Based on the following theorem, we establish the asymptotic validity of using imputed counterfactual outcomes and LLM-generated confounders in conditional independence testing.

Theorem 1. *Under standard regularity conditions on the kernel function and the class of imputation distributions, the KCIT applied to imputed variables satisfies:*

$$\text{KCIT}((\hat{Y}^0, \hat{Y}^1), T \mid X, \hat{U}) = \text{KCIT}((Y^0, Y^1), T \mid X, U) + o_p(1),$$

where $o_p(1)$ denotes a term that converges to zero in probability as the sample size increases. Please kindly refer to the appendix for a detailed proof of this theorem.

3.5 Progressive Confounder Imputation Procedure

Up to present, we have introduced how to impute a single confounder and test its validity. However, in real-world scenarios, hidden confounding often arises from multiple factors and may involve a large number of latent variables. For example, treatment assignment in healthcare may be influenced by a combination of demographic factors, socioeconomic status, and behavioral traits [40, 16], many of which are difficult to observe in practice.

A naive approach is to generate multiple confounders simultaneously, but this often results in redundancy or semantic overlap among the generated variables. To address this, we propose the

Table 1: Overall comparison of treatment effect estimation performance on the Jobs and Twins datasets. For each base model, the best results across methods are highlighted.

Datasets	Jobs				Twins			
	In-sample		Out-sample		In-sample		Out-sample	
Test Types	ϵ_{ATT}	\mathcal{R}_{pol}	ϵ_{ATT}	\mathcal{R}_{pol}	ϵ_{ATE}	ϵ_{PEHE}	ϵ_{ATE}	ϵ_{PEHE}
S-Learner	0.0491 \pm 0.0011	0.2289 \pm 0.0008	0.0876 \pm 0.0018	0.1678 \pm 0.0002	0.0131 \pm 0.0020	0.2527 \pm 0.0012	0.0037 \pm 0.0024	0.2819 \pm 0.0001
+ProCI-4o	0.0793 \pm 0.0043	0.2288 \pm 0.0001	0.0833 \pm 0.0001	0.1667 \pm 0.0014	0.0057 \pm 0.0000	0.2524 \pm 0.0001	0.0077 \pm 0.0000	0.2867 \pm 0.0003
+ProCI-R1	0.0216 \pm 0.0002	0.2324 \pm 0.0000	0.0712 \pm 0.0001	0.1745 \pm 0.0002	0.0066 \pm 0.0008	0.2596 \pm 0.0001	0.0028 \pm 0.0009	0.2817 \pm 0.0004
PSM	0.6197 \pm 0.0000	0.2707 \pm 0.0000	0.1259 \pm 0.0015	0.2192 \pm 0.0013	0.0457 \pm 0.0006	0.3399 \pm 0.0007	0.0840 \pm 0.0000	0.4027 \pm 0.0001
+ProCI-4o	0.6149 \pm 0.0001	0.2691 \pm 0.0017	0.1125 \pm 0.0032	0.2219 \pm 0.0002	0.0454 \pm 0.0051	0.3396 \pm 0.0004	0.0825 \pm 0.0021	0.4002 \pm 0.0011
+ProCI-R1	0.6245 \pm 0.0000	0.2633 \pm 0.0000	0.1292 \pm 0.0041	0.2163 \pm 0.0131	0.0454 \pm 0.0040	0.3399 \pm 0.0027	0.0849 \pm 0.0009	0.4033 \pm 0.0125
TARNet	0.0191 \pm 0.0002	0.2177 \pm 0.0001	0.1466 \pm 0.0026	0.2201 \pm 0.0002	0.0233 \pm 0.0044	0.2917 \pm 0.0001	0.0310 \pm 0.0005	0.3237 \pm 0.0001
+ProCI-4o	0.0424 \pm 0.0023	0.2167 \pm 0.0022	0.3223 \pm 0.0098	0.2150 \pm 0.0202	0.0144 \pm 0.0218	0.2729 \pm 0.0017	0.0185 \pm 0.0001	0.3107 \pm 0.0206
+ProCI-R1	0.0131 \pm 0.0001	0.2266 \pm 0.0000	0.0656 \pm 0.0024	0.2111 \pm 0.0004	0.0159 \pm 0.0001	0.2844 \pm 0.0009	0.0243 \pm 0.0001	0.3172 \pm 0.0001
CFR-Wass	0.0355 \pm 0.0006	0.2150 \pm 0.0001	0.1487 \pm 0.0028	0.2191 \pm 0.0004	0.0189 \pm 0.0000	0.2818 \pm 0.0000	0.0186 \pm 0.0002	0.3138 \pm 0.0000
+ProCI-4o	0.0300 \pm 0.0009	0.2085 \pm 0.0001	0.0402 \pm 0.0003	0.2151 \pm 0.0005	0.0094 \pm 0.0001	0.2729 \pm 0.0001	0.0178 \pm 0.0001	0.3110 \pm 0.0001
+ProCI-R1	0.0303 \pm 0.0010	0.2264 \pm 0.0042	0.1141 \pm 0.0067	0.2088 \pm 0.0004	0.0215 \pm 0.0002	0.2796 \pm 0.0061	0.0282 \pm 0.0003	0.3119 \pm 0.0032
ESCFR	0.0543 \pm 0.0012	0.2184 \pm 0.0001	0.2245 \pm 0.0390	0.2274 \pm 0.0002	0.0199 \pm 0.0001	0.2715 \pm 0.0001	0.0207 \pm 0.0003	0.3059 \pm 0.0007
+ProCI-4o	0.0369 \pm 0.0004	0.2174 \pm 0.0001	0.3225 \pm 0.0622	0.1891 \pm 0.0002	0.0191 \pm 0.0001	0.2700 \pm 0.0032	0.0297 \pm 0.0029	0.3045 \pm 0.0001
+ProCI-R1	0.0130 \pm 0.0001	0.2219 \pm 0.0000	0.1294 \pm 0.0072	0.2101 \pm 0.0008	0.0087 \pm 0.0001	0.2684 \pm 0.0002	0.0132 \pm 0.0001	0.3038 \pm 0.0000

complete ProCI framework, which incrementally generates confounders in a stepwise manner based on previously generated variables, ensuring diversity and sufficiency.

Formally, let $X^{(0)} = X$ denote the initial set of observed covariates. At each iteration k , we query the LLM using the current context $(X^{(k-1)}, T, Y)$ to produce a new confounder \hat{U} , and update the augmented confounder set as:

$$\hat{U}, \hat{U}_{\text{exp}} = \text{LLM}(\mathcal{P}_{\text{var}}(X^{(k-1)}, T, Y)), \quad X^{(k)} = [X^{(k-1)}, \hat{U}]. \quad (10)$$

After each generation step, we apply the empirical unconfoundedness test described in Eq. (15) to assess whether the updated set $X^{(k)}$ sufficiently captures all relevant confounding information. The process terminates at the smallest iteration k such that $X^{(k)}$ passes the test:

$$\min \left\{ k \mid \text{KCIT}((\hat{Y}^0, \hat{Y}^1), T \mid X^{(k)}) > \alpha \right\}. \quad (11)$$

That is, ProCI terminates precisely when the current set of confounders becomes sufficient for unbiased treatment effect estimation, avoiding both redundancy and under-adjustment.

4 Experiments

In this section, we conduct experiments to evaluate the effectiveness of the ProCI framework, guided by the following research questions: **[RQ1]** Can imputed confounders from different LLMs improve treatment effect estimation? **[RQ2]** Do the imputed confounders capture additional confounding information beyond observed covariates? **[RQ3]** Is ProCI robust to varying levels of hidden confounding? **[RQ4]** What is the contribution of each ProCI component?

4.1 Experimental Setup

Datasets. We evaluate on two commonly-used causal benchmarks: **Twins** [3] and **Jobs** [29]. **Twins** contains 8,244 twin pairs from U.S. birth records, with treatment indicating the heavier twin and outcome measuring one-year mortality. The dataset includes 50 demographic and birth-related covariates. Selection bias is introduced following [34]. **Jobs** studies the effect of a job training program on employment status. It includes 297 treated individuals, 425 randomized controls, and 2,490 observational controls, with 7 covariates describing demographic and economic features.

Base Models. ProCI augments observed data with generated confounders and thus is model-agnostic. We evaluate it with: (i) meta-learners (**S-Learner** [28]); (ii) matching-based methods (**PSM** [8]); and

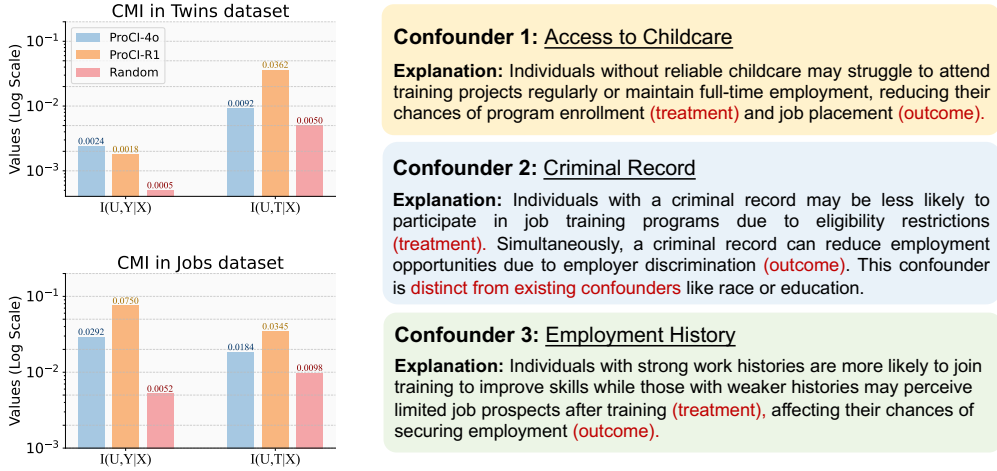


Figure 3: (Left) CMI measures dependence between LLM-generated confounders and treatment/outcome, compared to random confounders. (Right) Confounders generated in Jobs demonstrate their semantic relevance and impact on treatment/outcome.

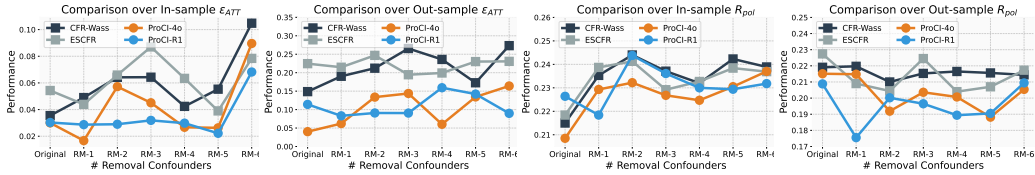


Figure 4: Robustness of ProCI in CATE estimation with varying hidden confounder removal.

(iii) representation learning models (**TARNet**, **CFR-Wass** [46], and **ESCFR** [51]). For confounder generation, we use two advanced LLMs: **GPT-4o** [21] and **DeepSeek-R1** [17].

Training & Evaluation Protocols. We use grid search for hyperparameter tuning on validation sets, and adopt consistent settings across shared base models. LLM temperature is fixed at 0.7. All models are implemented in PyTorch 1.10 and trained with Adam optimizer. For both datasets, we split the data into training, validation, and test sets (63:27:10 for Twins, 56:24:20 for Jobs). Twins is evaluated using ϵ_{PEHE} and ϵ_{ATE} [20], while Jobs uses ϵ_{ATT} and policy risk (\mathcal{R}_{pol}) [46] for evaluation. Please kindly refer to the appendix for more experimental details.

4.2 [RQ1] CATE Performance with Imputed Confounders

To answer RQ1, we apply our proposed ProCI framework using two LLMs, GPT-4o and DeepSeek-R1, denoted as ProCI-4o and ProCI-R1 respectively. We evaluate both variants across a diverse set of base CATE estimators. Each experiment is repeated five times to ensure stability.

Results. As shown in Table 1, we can see: *i*) ProCI-augmented estimators consistently outperform base models in both in-sample and out-of-sample settings, demonstrating the effectiveness of our imputed confounders. *ii*) All base model categories benefit from ProCI, with representation-based methods gaining the most, likely due to improved latent variable balancing. *iii*) ProCI-R1 generally outperforms ProCI-4o, indicating that DeepSeek-R1’s stronger reasoning leads to more accurate confounder generation and better bias correction.

4.3 [RQ2] Confounding Information in Imputed Confounders

To answer RQ2, we evaluate whether the confounders imputed by ProCI contain additional information beyond observed covariates. We use conditional mutual information (CMI) to measure the dependency of imputed confounders U with treatment T and outcome Y given observed variables X , i.e., $I(U, T|X)$ and $I(U, Y|X)$. Higher CMI values indicate more relevant confounding information.

Results. Figure 3 (left) compares imputed confounders from ProCI variants using GPT-4o and DeepSeek-R1 against random confounders generation baseline. The notably higher CMI values con-

firm that ProCI’s confounders carry significant additional information about treatment and outcome beyond observed covariates. In addition, Figure 3 (right) shows three example confounders generated by DeepSeek-R1 on Jobs. These confounders have plausible links to treatment and outcomes and are distinct from observed covariates, highlighting ProCI’s ability to uncover meaningful latent confounders omitted by traditional data.

4.4 [RQ3] Robustness of ProCI to Hidden Confounding

In this section, we evaluate the robustness of CATE estimators under hidden confounders. Since hidden confounders are unobservable, we simulate their effects by progressively removing $\{0, 1, 2, 3, 4, 5, 6\}$ confounders from the original dataset. This allows us to mimic the impact of latent confounders in a controlled manner. We experiment on Jobs and select CFR-Wass as base model.

Results. As shown in Figure 4, when the number of removed confounders increases, the performance of vanilla CATE estimators CFR-Wass and ESCFR degrades significantly across all metrics. This is expected, since these models are vulnerable to hidden confounder bias, leading to distorted CATE estimations. In contrast, our proposed ProCI framework maintains stable CATE estimation performance despite the progressive removal of confounders from the observed dataset. This robustness is attributed to ProCI’s progressive confounder generation capability, which introduces novel and informative confounders to counteract the sparsity induced by the removal of observed confounders.

4.5 [RQ4] Ablation Studies of ProCI Components

In this experiment, we conduct ablation studies to evaluate ProCI components. In specific, we tailor three variants: *i*) ProCI w/o DR, which removes distributional reasoning; *ii*) ProCI w/o PI, which eliminates the progressive manner in generating confounders; and *iii*) ProCI w/o UT, which omits the unconfoundedness test. Experiments are conducted on the Jobs dataset using GPT-4o as the LLM backbone.

Table 2: Results of ablation studies.

Methods	In-sample		Out-sample	
	ϵ_{ATT}	\mathcal{R}_{pol}	ϵ_{ATT}	\mathcal{R}_{pol}
w/o DR	0.0327	0.2178	0.1599	0.2229
w/o PI	0.0308	0.2223	0.1020	0.2374
w/o UT	0.0315	0.2218	0.0890	0.2270
ProCI	0.0300	0.2085	0.0402	0.2151

Results. Table 2 shows that removing any component from ProCI reduces performance. Specifically, removing distributional reasoning (w/o DR) leads to less robust estimations due to the corrupted values often generated by LLMs. Removing the progressive imputation process (w/o PI), where all confounders are generated at once, would inevitably introduces semantic overlap. Finally, omitting the unconfoundedness test (w/o UT) can include irrelevant confounders, further degrading the performance of ProCI.

5 Related Works

Treatment Effect Estimation with Hidden Confounding. To mitigate hidden confounding, existing approaches generally fall into three categories. Sensitivity analysis methods [43, 42] assess the potential effect of hidden confounders by deriving bounds on treatment effect estimates, though they rely on fixed, unverifiable assumptions [12, 50]. Auxiliary variable techniques, including instrumental variables and front-door adjustments [30, 13, 45], exploit external or intermediate variables to achieve unbiased estimates, but these depend on unverifiable structural assumptions [24, 53, 7]. Another line of work integrates RCTs with observational data [27, 19, 55] to correct for hidden biases, but their applicability is often constrained by the high costs and limited availability of RCT data.

LLMs for treatment effect estimation. LLMs have recently been explored for causal inference tasks [33, 57, 9, 31, 52, 48, 10, 32], especially in estimating treatment effects through prompt-based reasoning [1, 26, 36, 11, 23]. These methods typically focus on extracting causal structures from text or guiding LLMs to simulate interventional queries via carefully crafted prompts. For example, recent works use self-consistency [1], tool augmentation [36], and chain-of-thought prompting [26] to improve causal variable identification and treatment effect estimation. [11] further automates treatment effect estimation by combining LLM outputs with traditional treatment effect estimators.

6 Conclusion

In this work, we make the first attempt to leverage LLMs to mitigate hidden confounding in treatment effect estimation. We propose ProCI, a framework that progressively elicits LLMs to generate, impute, and validate hidden confounders using both structured and unstructured information. By incorporating distribution-aware imputation and an empirical unconfoundedness test grounded in the world knowledge embedded in LLMs, ProCI provides a robust and scalable solution for treatment effect estimation under hidden confounding. Extensive experiments across diverse datasets and LLMs demonstrate the effectiveness of our approach. This work offers a new perspective on using LLMs as knowledge-rich tools for treatment effect estimation under hidden confounding.

References

- [1] Sara Abdali, Anjali Parikh, Steve Lim, and Emre Kiciman. Extracting self-consistent causal insights from users feedback with llms and in-context learning. *arXiv preprint arXiv:2312.06820*, 2023.
- [2] Jason Abrevaya, Yu-Chin Hsu, and Robert P Lieli. Estimating conditional average treatment effects. *Journal of Business & Economic Statistics*, 33(4):485–505, 2015.
- [3] Douglas Almond, Kenneth Y Chay, and David S Lee. The costs of low birth weight. *The Quarterly Journal of Economics*, 120(3):1031–1083, 2005.
- [4] Arash A Amini and Zahra S Razaee. Concentration of kernel matrices with application to kernel spectral clustering. *The Annals of Statistics*, 49(1):531–556, 2021.
- [5] Cv Ananth and E. F. Schisterman. Hidden biases in observational epidemiology: the case of unmeasured confounding. *BJOG: An International Journal of Obstetrics & Gynaecology*, 125:644 – 646, 2018.
- [6] Serge Assaad, Shuxi Zeng, Chenyang Tao, Shounak Datta, Nikhil Mehta, Ricardo Henao, Fan Li, and Lawrence Carin. Counterfactual representation learning with balancing weights. In *International Conference on Artificial Intelligence and Statistics*, pages 1972–1980. PMLR, 2021.
- [7] Marc F. Bellemare, Jeffrey R. Bloem, and Noah Wexler. The paper of how: Estimating treatment effects using the front-door criterion*. *Oxford Bulletin of Economics and Statistics*, 2024.
- [8] Marco Caliendo and Sabine Kopeinig. Some practical guidance for the implementation of propensity score matching. *Journal of economic surveys*, 22(1):31–72, 2008.
- [9] Meiqi Chen, Yixin Cao, Yan Zhang, and Chaochao Lu. Quantifying and mitigating unimodal biases in multimodal large language models: A causal perspective. *arXiv preprint arXiv:2403.18346*, 2024.
- [10] Sirui Chen, Bo Peng, Meiqi Chen, Ruiqi Wang, Mengying Xu, Xingyu Zeng, Rui Zhao, Shengjie Zhao, Yu Qiao, and Chaochao Lu. Causal evaluation of language models. *arXiv preprint arXiv:2405.00622*, 2024.
- [11] Nikita Dhawan, Leonardo Cotta, Karen Ullrich, Rahul G Krishnan, and Chris J Maddison. End-to-end causal effect estimation from unstructured natural language data. *arXiv preprint arXiv:2407.07018*, 2024.
- [12] Alexander M. Franks, Alexander D’Amour, and Avi Feller. Flexible sensitivity analysis for observational studies without observable implications. *Journal of the American Statistical Association*, 115:1730 – 1746, 2018.
- [13] Isabel R. Fulcher, Ilya Shpitser, Stella Marealle, and Eric J. Tchetgen Tchetgen. Robust inference on population indirect causal effects: the generalized front door criterion. *Journal of the Royal Statistical Society: Series B (Statistical Methodology)*, 82, 2017.
- [14] Markus Gangl. Causal inference in sociological research. *Annual review of sociology*, 36(1):21–47, 2010.

- [15] Aaron Grattafiori, Abhimanyu Dubey, Abhinav Jauhri, Abhinav Pandey, Abhishek Kadian, Ahmad Al-Dahle, Aiesha Letman, Akhil Mathur, Alan Schelten, Alex Vaughan, et al. The llama 3 herd of models. *arXiv preprint arXiv:2407.21783*, 2024.
- [16] Paul Grootendorst. A review of instrumental variables estimation of treatment effects in the applied health sciences. *Health Services and Outcomes Research Methodology*, 7:159–179, 2007.
- [17] Daya Guo, Dejian Yang, Haowei Zhang, Junxiao Song, Ruoyu Zhang, Runxin Xu, Qihao Zhu, Shirong Ma, Peiyi Wang, Xiao Bi, et al. Deepseek-r1: Incentivizing reasoning capability in llms via reinforcement learning. *arXiv preprint arXiv:2501.12948*, 2025.
- [18] Kairong Han, Kun Kuang, Ziyu Zhao, Junjian Ye, and Fei Wu. Causal agent based on large language model. *arXiv preprint arXiv:2408.06849*, 2024.
- [19] Tobias Hatt, Jeroen Berrevoets, Alicia Curth, Stefan Feuerriegel, and Mihaela van der Schaar. Combining observational and randomized data for estimating heterogeneous treatment effects. *ArXiv*, abs/2202.12891, 2022.
- [20] Jennifer L Hill. Bayesian nonparametric modeling for causal inference. *Journal of Computational and Graphical Statistics*, 20(1):217–240, 2011.
- [21] Aaron Hurst, Adam Lerer, Adam P Goucher, Adam Perelman, Aditya Ramesh, Aidan Clark, AJ Ostrow, Akila Welihinda, Alan Hayes, Alec Radford, et al. Gpt-4o system card. *arXiv preprint arXiv:2410.21276*, 2024.
- [22] Alihan Hüyük, Xinnuo Xu, Jacqueline Maasch, Aditya V Nori, and Javier González. Reasoning elicitation in language models via counterfactual feedback. *arXiv preprint arXiv:2410.03767*, 2024.
- [23] Kosuke Imai and Kentaro Nakamura. Causal representation learning with generative artificial intelligence: Application to texts as treatments, 2024.
- [24] Guido Imbens. Instrumental variables: An econometrician’s perspective. *Political Methods: Quantitative Methods eJournal*, 2014.
- [25] Andrew Jesson, Sören Mindermann, Yarin Gal, and Uri Shalit. Quantifying ignorance in individual-level causal-effect estimates under hidden confounding. In *International Conference on Machine Learning*, pages 4829–4838. PMLR, 2021.
- [26] Zhijing Jin, Yuen Chen, Felix Leeb, Luigi Gresele, Ojasv Kamal, Zhiheng Lyu, Kevin Blin, Fernando Gonzalez Adatao, Max Kleiman-Weiner, Mrinmaya Sachan, et al. Cladder: Assessing causal reasoning in language models. *Advances in Neural Information Processing Systems*, 36:31038–31065, 2023.
- [27] Nathan Kallus, Ahlrad Puli, and Uri Shalit. Removing hidden confounding by experimental grounding. *ArXiv*, abs/1810.11646, 2018.
- [28] Sören R Künnel, Jasjeet S Sekhon, Peter J Bickel, and Bin Yu. Metalearners for estimating heterogeneous treatment effects using machine learning. *Proceedings of the national academy of sciences*, 116(10):4156–4165, 2019.
- [29] Robert J LaLonde. Evaluating the econometric evaluations of training programs with experimental data. *The American economic review*, pages 604–620, 1986.
- [30] Haoxuan Li, Kunhan Wu, Chunyuan Zheng, Yanghao Xiao, Hao Wang, Zhi Geng, Fuli Feng, Xiangnan He, and Peng Wu. Removing hidden confounding in recommendation: A unified multi-task learning approach. In *Neural Information Processing Systems*, 2023.
- [31] Victoria Lin, Eli Ben-Michael, and Louis-Philippe Morency. Optimizing language models for human preferences is a causal inference problem. *arXiv preprint arXiv:2402.14979*, 2024.
- [32] Victoria Lin, Louis-Philippe Morency, and Eli Ben-Michael. Text-transport: Toward learning causal effects of natural language. *arXiv preprint arXiv:2310.20697*, 2023.

- [33] Chenxi Liu, Yongqiang Chen, Tongliang Liu, Mingming Gong, James Cheng, Bo Han, and Kun Zhang. Discovery of the hidden world with large language models, 2024.
- [34] Christos Louizos, Uri Shalit, Joris M Mooij, David Sontag, Richard Zemel, and Max Welling. Causal effect inference with deep latent-variable models. *Advances in neural information processing systems*, 30, 2017.
- [35] Jing Ma. Causal inference with large language model: A survey. *arXiv preprint arXiv:2409.09822*, 2024.
- [36] Nick Pawlowski, James Vaughan, Joel Jennings, and Cheng Zhang. Answering causal questions with augmented llms. 2023.
- [37] Judea Pearl. Causal inference in statistics: An overview. *Statistics Surveys*, 3:96–146, 2009.
- [38] Judea Pearl and Dana Mackenzie. *The book of why: the new science of cause and effect*. Basic books, 2018.
- [39] Roman Pogodin, Antonin Schrab, Yazhe Li, Danica J. Sutherland, and Arthur Gretton. Practical kernel tests of conditional independence, 2024.
- [40] Mattia Proserpi, Yi Guo, Matt Sperrin, James S Koopman, Jae S Min, Xing He, Shannan Rich, Mo Wang, Iain E Buchan, and Jiang Bian. Causal inference and counterfactual prediction in machine learning for actionable healthcare. *Nature Machine Intelligence*, 2(7):369–375, 2020.
- [41] Qwen, :, An Yang, Baosong Yang, Beichen Zhang, Binyuan Hui, Bo Zheng, Bowen Yu, Chengyuan Li, Dayiheng Liu, Fei Huang, Haoran Wei, Huan Lin, Jian Yang, Jianhong Tu, Jianwei Zhang, Jianxin Yang, Jiaxi Yang, Jingren Zhou, Junyang Lin, Kai Dang, Keming Lu, Keqin Bao, Kexin Yang, Le Yu, Mei Li, Mingfeng Xue, Pei Zhang, Qin Zhu, Rui Men, Runji Lin, Tianhao Li, Tianyi Tang, Tingyu Xia, Xingzhang Ren, Xuancheng Ren, Yang Fan, Yang Su, Yichang Zhang, Yu Wan, Yuqiong Liu, Zeyu Cui, Zhenru Zhang, and Zihan Qiu. Qwen2.5 technical report, 2025.
- [42] Richard W. Robins, Avshalom Caspi, and Terrie E. Moffitt. Two personalities, one relationship: both partners’ personality traits shape the quality of their relationship. *Journal of personality and social psychology*, 79 2:251–9, 2000.
- [43] Paul R. Rosenbaum and Donald B. Rubin. Assessing sensitivity to an unobserved binary covariate in an observational study with binary outcome. *Journal of the royal statistical society series b-methodological*, 45:212–218, 1983.
- [44] Donald B Rubin. Causal inference using potential outcomes: Design, modeling, decisions. *Journal of the American statistical Association*, 100(469):322–331, 2005.
- [45] Abhin Shah, Karthikeyan Shanmugam, and Murat Kocaoglu. Front-door adjustment beyond markov equivalence with limited graph knowledge. *ArXiv*, abs/2306.11008, 2023.
- [46] Uri Shalit, Fredrik D Johansson, and David Sontag. Estimating individual treatment effect: generalization bounds and algorithms. In *International conference on machine learning*, pages 3076–3085. PMLR, 2017.
- [47] Zexu Sun, Hao Yang, Dugang Liu, Yunpeng Weng, Xing Tang, and Xiuqiang He. End-to-end cost-effective incentive recommendation under budget constraint with uplift modeling. In *Proceedings of the 18th ACM Conference on Recommender Systems*, pages 560–569, 2024.
- [48] Juanhe TJ Tan. Causal abstraction for chain-of-thought reasoning in arithmetic word problems. In *Proceedings of the 6th BlackboxNLP Workshop: Analyzing and Interpreting Neural Networks for NLP*, pages 155–168, 2023.
- [49] Hal R Varian. Causal inference in economics and marketing. *Proceedings of the National Academy of Sciences*, 113(27):7310–7315, 2016.
- [50] Victor Veitch and Anisha Zaveri. Sense and sensitivity analysis: Simple post-hoc analysis of bias due to unobserved confounding. *ArXiv*, abs/2003.01747, 2020.

- [51] Hao Wang, Jiajun Fan, Zhichao Chen, Haoxuan Li, Weiming Liu, Tianqiao Liu, Quanyu Dai, Yichao Wang, Zhenhua Dong, and Ruiming Tang. Optimal transport for treatment effect estimation. In *Thirty-seventh Conference on Neural Information Processing Systems*, 2023.
- [52] Jason Wei, Xuezhi Wang, Dale Schuurmans, Maarten Bosma, Fei Xia, Ed Chi, Quoc V Le, Denny Zhou, et al. Chain-of-thought prompting elicits reasoning in large language models. *Advances in neural information processing systems*, 35:24824–24837, 2022.
- [53] Anpeng Wu, Kun Kuang, B. Li, and Fei Wu. Instrumental variable regression with confounder balancing. In *International Conference on Machine Learning*, 2022.
- [54] Anpeng Wu, Kun Kuang, Ruoxuan Xiong, Bo Li, and Fei Wu. Stable estimation of heterogeneous treatment effects. In *International Conference on Machine Learning*, pages 37496–37510. PMLR, 2023.
- [55] Lili Wu and Shu Yang. Integrative r-learner of heterogeneous treatment effects combining experimental and observational studies. In *CLEaR*, 2022.
- [56] Liuyi Yao, Sheng Li, Yaliang Li, Mengdi Huai, Jing Gao, and Aidong Zhang. Representation learning for treatment effect estimation from observational data. *Advances in neural information processing systems*, 31, 2018.
- [57] Shitian Zhao, Zhuowan Li, Yadong Lu, Alan Yuille, and Yan Wang. Causal-cog: A causal-effect look at context generation for boosting multi-modal language models. In *Proceedings of the IEEE/CVF Conference on Computer Vision and Pattern Recognition*, pages 13342–13351, 2024.

A In-Depth Causal Inference Preliminaries

This section provides additional background on causal inference, which is particularly intended to assist readers who may be less familiar with the foundational concepts or technical aspects of treatment effect estimation from observational data.

We begin by introducing key definitions and assumptions underlying causal inference from observational data. For an individual characterized by covariates x , there are two potential outcomes: Y^1 if the individual receives treatment and Y^0 if assigned to control. The Conditional Average Treatment Effect (CATE) captures the expected difference in outcomes between these two scenarios:

Definition 1. *The CATE for individuals with covariates x is defined as*

$$\tau(x) = \mathbb{E}[Y^1 - Y^0 \mid X = x], \quad (12)$$

where X denotes the covariate variable, and Y^1, Y^0 are the potential outcomes under treatment and control, respectively.

Estimating CATE from observational data poses two primary challenges:

1. *Missing counterfactuals:* For each individual, we only observe the outcome corresponding to the assigned treatment. The unobserved counterfactual remains inaccessible.
2. *Selection bias:* Treatment assignment may depend on covariates related to the outcome, leading to systematic differences between treated and control groups.

To address these challenges, [38] proposed a two-stage framework. The first stage, *identification*, aims to express causal quantities, such as $\tau(x)$, in terms of observed data using assumptions and adjustment formulas. Identification is not always guaranteed, and depends on the following assumptions:

Assumption 2 (Ignorability / Unconfoundedness). *The treatment assignment is independent of the potential outcomes given the covariates, i.e., $Y^1, Y^0 \perp\!\!\!\perp T \mid X = x$.*

Assumption 3 (Positivity). *For any value x , both treatment and control must have non-zero probability, i.e., $0 < P(T = t \mid X = x) < 1$ for all $t \in \{0, 1\}$.*

Assumption 4 (SUTVA). *The potential outcomes for any individual are unaffected by others' treatment assignments, and each treatment corresponds to a single well-defined outcome.*

Assumption 5 (Consistency). *The observed outcome equals the potential outcome under the treatment actually received.*

Once identification is established, the second stage, *estimation*, transforms the causal estimand into a statistical estimand that can be computed from the data:

$$\begin{aligned} \mathbb{E}[Y^1 - Y^0 \mid X = x] &= \mathbb{E}[Y^1 \mid X = x] - \mathbb{E}[Y^0 \mid X = x] \\ &\stackrel{(1)}{=} \mathbb{E}[Y^1 \mid X = x, T = 1] - \mathbb{E}[Y^0 \mid X = x, T = 0] \\ &\stackrel{(2)}{=} \mathbb{E}[Y \mid X = x, T = 1] - \mathbb{E}[Y \mid X = x, T = 0], \end{aligned} \quad (13)$$

where step (1) uses Assumption 2, and step (2) additionally relies on Assumptions 3, 4, and 5.

In practice, numerous approaches have been developed to estimate the last quantity. Classical methods include matching strategies [8], which pair treated and control units with similar covariates, and meta-learners [28], which adapt supervised learning techniques to causal inference tasks. More recent advances leverage deep learning, notably representation learning methods [6, 54], which aim to mitigate selection bias by learning balanced latent spaces. A prominent example is Counterfactual Regression (CFR) [46], which introduces regularization terms based on distributional distances—such as the Wasserstein distance or the maximum mean discrepancy—to align representations between treatment groups.

Despite their success, these approaches heavily rely on the unconfoundedness assumption, which is often violated in real-world datasets where hidden confounding factors may influence both treatment and outcome. While some recent methods attempt to account for hidden confounding, they typically depend on strong structural assumptions, additional proxies, or access to experimental (RCT) data—which may be costly or unavailable in practice.

In this paper, we take a new direction by exploring the potential of large language models (LLMs) to assist in imputing latent confounders from observational text and tabular data. Specifically, we propose a framework ProCI that leverages LLMs' implicit knowledge and generative ability to infer proxy variables that encode hidden causal information—thus helping to relax the unconfoundedness assumption and improve the robustness of causal estimates in the presence of hidden confounding.

B Proof of Theorem 1

In Theorem 1, we aim to employ the kernel-based conditional independence test (KCIT) to assess whether the potential outcomes are conditionally independent of the treatment variable, given both observed and latent covariates. Specifically, we test whether:

$$\mathbf{Y} = (Y^0, Y^1) \perp\!\!\!\perp T \mid X, U$$

Hypotheses.

- **Null Hypothesis** (H_0): $\mathbf{Y} \perp\!\!\!\perp T \mid X, U$ — the potential outcomes are conditionally independent of treatment given covariates.
- **Alternative Hypothesis** (H_1): $\mathbf{Y} \not\perp\!\!\!\perp T \mid X, U$ — there exists residual dependence between treatment and outcomes after conditioning on covariates.

Test Statistic. KCIT estimates the squared Hilbert-Schmidt norm of the partial cross-covariance operator between $\mathbf{Y} = (Y^0, Y^1)$ and T given (X, U) . Let n be the sample size. For two random vectors $X, Y \in \mathcal{X} \times \mathcal{Y}$, define the cross-variance operator as $\langle g, \Sigma_{YX} f \rangle = \mathbb{E}_{XY}(f(X)g(Y)) - \mathbb{E}_X f(X)\mathbb{E}_Y g(Y)$ for $f \in \mathcal{H}_X$ and $g \in \mathcal{H}_Y$, the RKHS of \mathcal{X} and \mathcal{Y} respectively. The cross-variance operator is estimated via $\hat{\Sigma}_{YX} = \frac{1}{n} \text{Tr}(\tilde{K}_X \tilde{K}_Y)$, with $\tilde{K}_X = HK_X H$, $H = I - \frac{1}{n} \mathbf{1}\mathbf{1}^\top$ and the (i, j) -th entry of K_X is $k(x_i, x_j)$. The KCIT operator is estimated via:

$$\hat{\Sigma}_{\mathbf{Y}T|(X,U)} = \hat{\Sigma}_{\mathbf{Y}T} - \hat{\Sigma}_{\mathbf{Y}Z}(\hat{\Sigma}_{ZZ} + \gamma I)^{-1} \hat{\Sigma}_{ZT} \quad (14)$$

with $Z = (X, U)$, and $\gamma > 0$ is a regularization parameter. Finally, the KCIT test statistics is constructed by

$$\text{KCIT}(\mathbf{Y}, T \mid (X, U)) = \frac{1}{n} \text{Tr}(\hat{\Sigma}_{\mathbf{Y}T|(X,U)}). \quad (15)$$

Lemma 1 (Theorem 1 in [4]). *Let $X_i \in \text{LC}(\mu_i, \Sigma_i, \omega)$, $i = 1, \dots, n$, be a collection of independent random vectors from the LC distribution class defined in [4], and let $K = K(X)$ be the kernel matrix for an L -Lipschitz kernel function $k(x_1, x_2)$, i.e. $|k(x_1, x_2) - k(y_1, y_2)| \leq L(\|x_1 - y_1\| + \|x_2 - y_2\|)$. Then, for some universal constant $c > 0$, with probability at least $1 - \exp(-ct^2)$,*

$$\|K - \mathbb{E}K\| \leq 2L\omega\sigma_\infty(Cn + \sqrt{nt}),$$

where $\sigma_\infty^2 := \max_i \|\Sigma_i\|$ and $C = c^{-1/2}$.

Lemma 2. *Let \hat{Y}_i, \hat{Z}_i be samples from LC classes $\text{LC}(\mu_Y, \Sigma_{Y_i}, \omega)$ and $\text{LC}(\mu_Z, \Sigma_{Z_i}, \omega)$ respectively³, such that $\|\mathbb{E}\tilde{K}_{\hat{Y}} - \tilde{K}_Y\| = o_p(1)$ and $\|\mathbb{E}\tilde{K}_{\hat{Z}} - \tilde{K}_Z\| = o_p(1)$. Then, for Gaussian RBF such that $\sigma \rightarrow \infty$ as $n \rightarrow \infty$, we have*

$$\begin{aligned} \|\hat{\Sigma}_{\hat{Y}T} - \hat{\Sigma}_{YT}\| &= o_p(1) \\ \|\hat{\Sigma}_{\hat{Y}\hat{Z}} - \hat{\Sigma}_{YZ}\| &= o_p(1) \\ \|\hat{\Sigma}_{\hat{Z}T} - \hat{\Sigma}_{ZT}\| &= o_p(1) \\ \|\hat{\Sigma}_{\hat{Z}\hat{Z}} - \hat{\Sigma}_{ZZ}\| &= o_p(1) \end{aligned} \quad (16)$$

with the last equation implies $\|\hat{\Sigma}_{\hat{Z}\hat{Z}}^{-1} - \hat{\Sigma}_{ZZ}^{-1}\| = o_p(1)$.

Proof of Lemma 2. From Lemma 1, with probability at least $1 - \exp(-ct^2)$,

$$\|K_{\hat{Y}} - \mathbb{E}K_{\hat{Y}}\| \leq 2L\omega\sigma_\infty(Cn + \sqrt{nt}).$$

³Here $\hat{Z} = (X, \hat{U})$, where \hat{U} is the estimation of latent confounders.

Therefore, since $L = o(\sigma^{-1}) = o(1)$ as n tends to infinity, $\|\tilde{K}_{\hat{Y}} - \mathbb{E}\tilde{K}_{\hat{Y}}\| \leq \|H\|^2 \|K_{\hat{Y}} - \mathbb{E}K_{\hat{Y}}\| = o_p(n)$. From above we have

$$\begin{aligned} \|\hat{\Sigma}_{\hat{Y}T} - \hat{\Sigma}_{YT}\| &= \frac{1}{n} \text{Tr}(\tilde{K}_X(\tilde{K}_{\hat{Y}} - \tilde{K}_Y)) \\ &\leq \frac{1}{n} \|\tilde{K}_X\| \cdot \|\tilde{K}_{\hat{Y}} - \tilde{K}_Y\| \\ &\leq \frac{1}{n} \|\tilde{K}_X\| \cdot (\|\tilde{K}_{\hat{Y}} - \mathbb{E}\tilde{K}_{\hat{Y}}\| + \|\mathbb{E}\tilde{K}_{\hat{Y}} - \tilde{K}_Y\|) \\ &= o_p(1), \end{aligned}$$

which proves the first equation in Eq. (16). The second equation comes from the fact that

$$\begin{aligned} \|\hat{\Sigma}_{\hat{Y}\hat{Z}} - \hat{\Sigma}_{YZ}\| &= \frac{1}{n} \text{Tr}(\tilde{K}_{\hat{Y}}(\tilde{K}_{\hat{Z}} - \tilde{K}_Z) + \tilde{K}_Z(\tilde{K}_{\hat{Y}} - \tilde{K}_Y)) \\ &\leq \frac{1}{n} (\|\tilde{K}_{\hat{Y}}\| \cdot \|\tilde{K}_{\hat{Z}} - \tilde{K}_Z\| + \|\tilde{K}_Z\| \cdot \|\tilde{K}_{\hat{Y}} - \tilde{K}_Y\|) \\ &= o_p(1). \end{aligned}$$

with the last equation resulting from $\|\tilde{K}_{\hat{Y}} - \tilde{K}_Y\| = o_p(n)$ and $\|\tilde{K}_{\hat{Z}} - \tilde{K}_Z\| = o_p(n)$. The third equation in Eq. (16) comes from the same deduction as for the first equation, and the last equation comes from the same deduction for the second equation.

Finally, the conclusion on the inverse matrix is straightforward observing that

$$(\hat{\Sigma}_{\hat{Z}\hat{Z}} + \mathcal{E})^{-1} = \hat{\Sigma}_{\hat{Z}\hat{Z}}^{-1} - \hat{\Sigma}_{\hat{Z}\hat{Z}}^{-1} \mathcal{E} \hat{\Sigma}_{\hat{Z}\hat{Z}}^{-1} + O_p(\|\mathcal{E}\|) = \hat{\Sigma}_{\hat{Z}\hat{Z}}^{-1} + o_p(1)$$

with $\|\mathcal{E}\| = o_p(1)$. □

Theorem 2. *Under standard regularity conditions on the kernel function and the class of imputation distributions, the KCIT applied to imputed variables satisfies:*

$$\text{KCIT}((\hat{Y}^0, \hat{Y}^1), T \mid X, \hat{U}) = \text{KCIT}((Y^0, Y^1), T \mid X, U) + o_p(1),$$

where $o_p(1)$ denotes a term that converges to zero in probability as the sample size increases.

Proof of Theorem 1. Based on Lemma 2 and Eq. (14), we have

$$\begin{aligned} \hat{\Sigma}_{\hat{Y}T|\hat{Z}} &= \hat{\Sigma}_{\hat{Y}T} - \hat{\Sigma}_{\hat{Y}\hat{Z}}(\hat{\Sigma}_{\hat{Z}\hat{Z}} + \gamma I)^{-1} \hat{\Sigma}_{\hat{Z}T} \\ &= \hat{\Sigma}_{YT} - \hat{\Sigma}_{YZ}(\hat{\Sigma}_{ZZ} + \gamma I)^{-1} \hat{\Sigma}_{ZT} + o_p(1) \\ &= \hat{\Sigma}_{YT|Z} + o_p(1). \end{aligned}$$

Therefore, based on Eq. (15), we have

$$\begin{aligned} &|\text{KCIT}((Y^0, Y^1), T \mid X, U) - \text{KCIT}((\hat{Y}^0, \hat{Y}^1), T \mid X, \hat{U})| \\ &= \frac{1}{n} |\text{Tr}(\hat{\Sigma}_{\hat{Y}T|\hat{Z}} - \hat{\Sigma}_{YT|Z})| \\ &\leq \|\hat{\Sigma}_{\hat{Y}T|\hat{Z}} - \hat{\Sigma}_{YT|Z}\| \\ &= o_p(1), \end{aligned}$$

which proves the theorem.

C Further Experimental Details

C.1 Dataset

Twins. The Twins dataset is derived from all recorded twin births in the United States between 1989 and 1991 [3]. We focus on twin pairs where both individuals weighed less than 2000 grams at birth. Each instance contains 50 pre-treatment covariates related to parental characteristics, pregnancy

Table 3: Hyperparameter search space used in all experiments.

Hyperparameter	Search Range	Description
lr	$\{10^{-5}, 10^{-4}, 10^{-3}, 10^{-2}, 10^{-1}\}$	learning rate
bs	$\{16, 32, 64, 128\}$	batch size
λ	$\{10^{-4}, 10^{-3}, 10^{-2}, 10^{-1}, 1\}$	loss balancing coefficient
d_ϕ	$\{16, 32, 64\}$	hidden dimension in encoder network ϕ
d_h	$\{16, 32, 64\}$	hidden dimension in outcome heads h_0 and h_1

conditions, and birth outcomes. The treatment assignment is defined such that $T = 1$ corresponds to the heavier twin and $T = 0$ to the lighter one. The outcome variable Y is one-year mortality.

After removing records with missing values, the resulting dataset comprises 8,244 samples. Since data for both twins in each pair is available, we observe outcomes under both treatment assignments ($T = 0$ and $T = 1$). To emulate an observational setting, we simulate unobserved counterfactuals by selectively masking one twin per pair. When this selection is randomized, the data mimics a randomized controlled trial. In specific, we model confounding via a proxy variable, where we assign treatment based on a single feature—GESTAT10—which represents gestational age in 10 categories. Formally, treatment is drawn as: $T_i | X_i, Z_i \sim \text{Bern}(\sigma(W_o^\top X_i + W_h(Z_i/10 - 0.1)))$, where $W_o \sim \mathcal{N}(0, 0.1 \cdot I)$ and $W_h \sim \mathcal{N}(5, 0.1)$. Here, X_i denotes the 49 non-GESTAT10 features and Z_i is the GESTAT10 value for unit i .

Jobs. This dataset combines the Lalonde randomized experiment (297 treated and 425 control units) with an observational sample from the PSID (2,490 control units) [29]. Each record includes 7 covariates such as age, education level, ethnicity, and prior earnings. The outcome reflects post-intervention employment status. By merging the experimental and observational subsets, we can introduce the selection bias between treated and control groups, making this dataset useful for evaluating robustness to such bias.

C.2 Training and Evaluation Protocols

Training Protocol. All models are optimized using grid search based on validation performance. The learning rate and batch size are tuned over predefined discrete sets: $\{10^{-5}, 10^{-4}, 10^{-3}, 10^{-2}, 10^{-1}\}$ for learning rates and $\{16, 32, 64, 128\}$ for batch sizes. For methods involving balancing losses (CFR-Wass, CFR-MMD, and ESCFR), the regularization weight λ is selected from $\{10^{-4}, 10^{-3}, 10^{-2}, 10^{-1}, 1\}$ to control the trade-off between outcome prediction and representation alignment. Table 3 summarizes the full hyperparameter configuration space used during training. All models, including the baselines and our proposed method, are tuned under the same conditions to ensure fair comparison.

Training is performed for a maximum of 200 epochs, with early stopping applied based on validation loss. Specifically, we stop the training process if no improvement is observed within 30 consecutive epochs, which helps prevent overfitting—particularly relevant for datasets like Twins, where ground-truth outcomes are fully known. All experiments are implemented using PyTorch 1.10 and trained with the Adam optimizer. Hardware used includes an NVIDIA A40 GPU and an Intel(R) Xeon(R) Gold 5318Y CPU at 2.10GHz.

Evaluation Protocol. For the Twins dataset, where the distributions of potential outcomes are available, we evaluate model performance using two metrics: the Precision in Estimation of Heterogeneous Effect (ϵ_{PEHE}) and the Average Treatment Effect error (ϵ_{ATE}) [20].

The PEHE is defined as:

$$\epsilon_{PEHE} = \frac{1}{N} \sum_{i=1}^N \left(\mathbb{E}_{(y_i^0, y_i^1) \sim \mathcal{P}_{\mathbf{X}|x_i}} (y_i^1 - y_i^0) - (\hat{y}_i^1 - \hat{y}_i^0) \right)^2,$$

where \hat{y}_i^0 and \hat{y}_i^1 denote the estimated outcomes under control and treatment, respectively, and y_i^0 and y_i^1 represent the corresponding true outcomes.

For the ATE error, we compute it as:

$$\epsilon_{ATE} = \left| \frac{1}{N} \sum_{i=1}^N (y_i^1 - y_i^0) - \frac{1}{N} \sum_{i=1}^N (\hat{y}_i^1 - \hat{y}_i^0) \right|.$$

Lower values of ϵ_{PEHE} and ϵ_{ATE} indicate better estimation performance.

For the Jobs dataset, where ground-truth ITE is not available, we use two metrics: policy risk \mathcal{R}_{pol} [46] and the error in estimating the Average Treatment effect on the Treated (ϵ_{ATT}).

Policy risk is defined as:

$$\mathcal{R}_{pol} = 1 - (\mathbb{E}[Y^1 | \pi(x) = 1] \cdot \mathbb{P}(\pi(x) = 1) + \mathbb{E}[Y^0 | \pi(x) = 0] \cdot \mathbb{P}(\pi(x) = 0)),$$

where $\pi(x) = 1$ if $\hat{y}^1 - \hat{y}^0 > 0$, and $\pi(x) = 0$ otherwise.

We estimate this metric using only units from the randomized component of the dataset:

$$\mathcal{R}_{pol} = 1 - \left(\frac{1}{|A^1 \cap T^1 \cap E|} \sum_{\mathbf{x}_i \in A^1 \cap T^1 \cap E} y_i^1 \cdot \frac{|A^1 \cap E|}{|E|} + \frac{1}{|A^0 \cap T^0 \cap E|} \sum_{\mathbf{x}_i \in A^0 \cap T^0 \cap E} y_i^0 \cdot \frac{|A^0 \cap E|}{|E|} \right) \quad (17)$$

with E denoting the randomized experiment set, $A^1 = \{\mathbf{x}_i : \hat{y}_i^1 - \hat{y}_i^0 > 0\}$, $A^0 = \{\mathbf{x}_i : \hat{y}_i^1 - \hat{y}_i^0 < 0\}$, $T^1 = \{\mathbf{x}_i : t_i = 1\}$, and $T^0 = \{\mathbf{x}_i : t_i = 0\}$. A lower value of \mathcal{R}_{pol} indicates that the CATE estimation method provides better support for the decision-making strategy.

We also report ϵ_{ATT} as:

$$\epsilon_{ATT} = \left| \frac{1}{N_1} \sum_{i:t_i=1} (y_i^1 - y_i^0) - \frac{1}{N_1} \sum_{i:t_i=1} (\hat{y}_i^1 - \hat{y}_i^0) \right|,$$

where N_1 is the number of treated units in the randomized group. A lower ϵ_{ATT} indicates more accurate treatment effect estimation for the treated population.

C.3 Base Models

Since our proposed ProCI framework is model-agnostic and only augments the original dataset with new confounders, it can be flexibly combined with a variety of existing CATE estimation methods. In our experiments, we treat several well-established and state-of-the-art CATE estimators as base models to assess how their performance improves when equipped with the confounders generated by ProCI.

We consider representative methods from three major categories: meta-learning, matching-based, and representation-based approaches.

i) Meta-learners: These methods differ in how they handle treatment information. The **S-Learner** [28] uses a single model that includes treatment as a feature.

ii) Matching-based methods: We include propensity score matching (**PSM**) [8], followed by regression on the matched samples. Propensity scores in PSM are estimated using logistic regression, consistent with the implementation in [8].

iii) Representation-based methods: This includes **TARNet** [46], which employs a shared feature representation with separate heads for predicting potential outcomes; **CFR-Wass** [46], which adds distributional regularization using the Wasserstein metric; and **ESCFR** [51], which leverages unbalanced optimal transport to achieve mini-batch-level representation balance and robustness to outliers.

Table 4: Overall performance comparison of treatment effect estimation between base models and their enhanced versions with ProCI-La (LLaMA 3-8B) and ProCI-Qw (Qwen2.5-7B). Best-performing results across all methods are highlighted.

Datasets	Jobs				Twins			
	In-sample		Out-sample		In-sample		Out-sample	
Test Types	ϵ_{ATT}	\mathcal{R}_{pol}	ϵ_{ATT}	\mathcal{R}_{pol}	ϵ_{ATE}	ϵ_{PEHE}	ϵ_{ATE}	ϵ_{PEHE}
Methods	ϵ_{ATT}	\mathcal{R}_{pol}	ϵ_{ATT}	\mathcal{R}_{pol}	ϵ_{ATE}	ϵ_{PEHE}	ϵ_{ATE}	ϵ_{PEHE}
S-Learner	0.0491 \pm 0.0011	0.2289 \pm 0.0008	0.0876 \pm 0.0018	0.1678 \pm 0.0002	0.0131 \pm 0.0020	0.2527 \pm 0.0012	0.0037 \pm 0.0024	0.2819 \pm 0.0001
+ProCI-La	0.0227 \pm 0.0004	0.2253 \pm 0.0013	0.1009 \pm 0.0001	0.1648 \pm 0.0002	0.0117 \pm 0.0001	0.2536 \pm 0.0000	0.0035 \pm 0.0029	0.2833 \pm 0.0032
+ProCI-Qw	0.0320 \pm 0.0007	0.2301 \pm 0.0000	0.0832 \pm 0.0001	0.1697 \pm 0.0010	0.0068 \pm 0.0013	0.2518 \pm 0.0027	0.0050 \pm 0.0004	0.2846 \pm 0.0012
PSM	0.6197 \pm 0.0000	0.2707 \pm 0.0000	0.1259 \pm 0.0015	0.2192 \pm 0.0013	0.0457 \pm 0.0006	0.3399 \pm 0.0007	0.0840 \pm 0.0000	0.4027 \pm 0.0001
+ProCI-La	0.6185 \pm 0.0008	0.2716 \pm 0.0003	0.1126 \pm 0.0002	0.2181 \pm 0.0001	0.0460 \pm 0.0012	0.3394 \pm 0.0004	0.0845 \pm 0.0000	0.4026 \pm 0.0000
+ProCI-Qw	0.6173 \pm 0.0000	0.2691 \pm 0.0001	0.0992 \pm 0.0003	0.2191 \pm 0.0035	0.0455 \pm 0.0037	0.3401 \pm 0.0000	0.0818 \pm 0.0001	0.4017 \pm 0.0000
TARNet	0.0191 \pm 0.0002	0.2177 \pm 0.0001	0.1466 \pm 0.0026	0.2201 \pm 0.0002	0.0233 \pm 0.0044	0.2917 \pm 0.0001	0.0310 \pm 0.0005	0.3237 \pm 0.0001
+ProCI-La	0.0163 \pm 0.0021	0.2059 \pm 0.0027	0.1179 \pm 0.0032	0.2139 \pm 0.0011	0.0190 \pm 0.0021	0.2755 \pm 0.0013	0.0270 \pm 0.0019	0.3043 \pm 0.0012
+ProCI-Qw	0.0129 \pm 0.0001	0.2005 \pm 0.0000	0.0761 \pm 0.0010	0.2201 \pm 0.0032	0.0101 \pm 0.0000	0.2775 \pm 0.0014	0.0092 \pm 0.0001	0.3123 \pm 0.0002
CFR-Wass	0.0355 \pm 0.0006	0.2150 \pm 0.0001	0.1487 \pm 0.0028	0.2191 \pm 0.0004	0.0189 \pm 0.0000	0.2818 \pm 0.0000	0.0186 \pm 0.0002	0.3138 \pm 0.0000
+ProCI-La	0.0312 \pm 0.0003	0.2023 \pm 0.0001	0.1373 \pm 0.0073	0.1986 \pm 0.0004	0.0132 \pm 0.0001	0.2762 \pm 0.0001	0.0150 \pm 0.0001	0.3073 \pm 0.0001
+ProCI-Qw	0.0295 \pm 0.0004	0.2029 \pm 0.0001	0.1389 \pm 0.0068	0.2140 \pm 0.0002	0.0137 \pm 0.0000	0.2724 \pm 0.0000	0.0110 \pm 0.0001	0.3041 \pm 0.0002
ESCFR	0.0543 \pm 0.0012	0.2184 \pm 0.0001	0.2245 \pm 0.0390	0.2274 \pm 0.0002	0.0199 \pm 0.0001	0.2715 \pm 0.0001	0.0207 \pm 0.0003	0.3059 \pm 0.0007
+ProCI-La	0.0362 \pm 0.0005	0.2074 \pm 0.0000	0.1218 \pm 0.0038	0.2055 \pm 0.0015	0.0160 \pm 0.0001	0.2714 \pm 0.0002	0.0177 \pm 0.0001	0.3030 \pm 0.0001
+ProCI-Qw	0.0317 \pm 0.0008	0.2154 \pm 0.0011	0.2114 \pm 0.0430	0.2239 \pm 0.0033	0.0131 \pm 0.0001	0.2699 \pm 0.0021	0.0062 \pm 0.0000	0.2989 \pm 0.0001

D Additional Experimental Results

D.1 Effectiveness of ProCI with Open-Source Language Models

Experimental Setup. To further investigate the generalizability of ProCI under different LLM architectures, we introduce two additional models: LLaMA 3–8B and Qwen2.5–7B, denoted as **ProCI-La** and **ProCI-Qw**, respectively. These models are selected for their competitive reasoning capabilities and open accessibility. ProCI-La is based on Meta’s LLaMA 3 series [15], a dense decoder-only transformer optimized for instruction-following. ProCI-Qw leverages Alibaba’s Qwen2.5 family [41], which has shown strong performance in multi-lingual and causal reasoning tasks.

We apply the same ProCI framework using LLaMA 3–8B and Qwen2.5–7B as the confounder generators. All settings (e.g., temperature = 0.7, prompt structure, distribution identification and imputation, progressive confounder generation) remain consistent with the original experiments to ensure fair comparisons. The resulting augmented datasets are then passed into the same downstream CATE estimators as in the original setup.

Results. As shown in Table 4, both ProCI-La and ProCI-Qw significantly improve CATE estimation performance over their corresponding base models, confirming the effectiveness of using LLM-generated hidden confounders even beyond proprietary GPT models. Notably, the improvements are consistent across different types of base estimators, with the following observations:

- **ProCI-La, based on LLaMA 3–8B, achieves strong performance gains on both in-sample and out-of-sample evaluations.** Its improvements are particularly evident when paired with representation-based base models such as TARNet and CFR-Wass, indicating that LLaMA 3’s semantic reasoning helps uncover latent variables that enhance feature balancing in the learned representations.
- **ProCI-Qw, leveraging Qwen2.5–7B, also brings stable improvements over base models.** While its performance slightly lags behind ProCI-La in some cases, it still consistently enhances treatment effect estimation, especially under models sensitive to unobserved confounding. This suggests Qwen2.5 can effectively contribute causal priors despite its smaller scale.
- **Across both models, we observe that representation learning-based estimators benefit the most from ProCI augmentation.** These models are designed to learn balanced representations of treated and control groups, and the inclusion of high-quality confounders improves this balancing, thereby reducing estimation bias and variance more effectively.

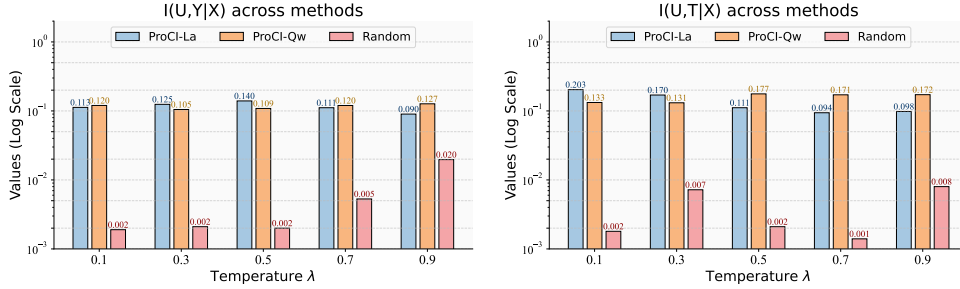


Figure 5: **Conditional mutual information (CMI) values across different temperatures for confounders generated by ProCI-La (LLaMA 3-8B), ProCI-Qw (Qwen2.5-7B), and a Random baseline.** The left plot shows $I(U, Y | X)$, and the right plot shows $I(U, T | X)$, with all values on a log scale. ProCI methods consistently outperform the Random baseline, with peak informativeness generally occurring at moderate temperatures (0.5–0.7).

These findings demonstrate that ProCI is model-agnostic and remains effective when paired with open-source, instruction-tuned LLMs. This extends its practical applicability and offers a cost-efficient, scalable solution for treatment effect estimation under hidden confounding in real-world settings.

D.2 Impact of Temperature on Confounder Quality

Experimental Setup. To assess how the temperature coefficient λ affects the quality of generated confounders, we conduct a controlled experiment using two open-source LLMs: **LLaMA 3-8B (ProCI-La)** and **Qwen2.5-7B (ProCI-Qw)**. We vary λ in the range $\{0.1, 0.3, 0.5, 0.7, 0.9\}$, and for each value, use the respective LLM to generate confounders following the standard ProCI framework. To evaluate the informativeness of the generated variables, we compute their conditional mutual information (CMI) with the treatment and outcome, conditioned on observed covariates: $I(U, Y | X)$ and $I(U, T | X)$. We also include a **Random** baseline that generates synthetic variables from uniform or Gaussian noise independent of the data. This helps isolate the contribution of semantically meaningful generation from LLMs.

Results. Figure 5 shows the CMI values $I(U, Y | X)$ and $I(U, T | X)$ across different temperature values. Each x-axis tick corresponds to a specific temperature coefficient λ , and we compare three methods: Random, ProCI-La, and ProCI-Qw.

- **ProCI-La and ProCI-Qw significantly outperform the Random baseline at all temperatures**, with CMI values often one to two orders of magnitude higher, validating that LLM-generated confounders encode semantically relevant information about treatment and outcome.
- **The impact of temperature varies by method and metric.** For $I(U, Y | X)$, ProCI-La achieves the highest value at $\lambda = 0.5$, while ProCI-Qw peaks at $\lambda = 0.9$. For $I(U, T | X)$, ProCI-La performs best at the lowest temperature ($\lambda = 0.1$), whereas ProCI-Qw shows more stable performance across mid-to-high temperatures.
- **ProCI-La generally outperforms ProCI-Qw in capturing outcome-relevant information**, especially at lower temperatures. In contrast, ProCI-Qw sometimes surpasses ProCI-La on treatment-related informativeness ($I(U, T | X)$), suggesting complementary strengths between the LLMs.

These findings reinforce the benefit of using temperature tuning to control the diversity and informativeness of generated confounders. Moderate values ($\lambda \in [0.5, 0.7]$) typically offer the best trade-off, with performance degrading slightly at the extremes.

E Prompt Templates

In this section, we present the detailed prompt templates used in the proposed ProCI framework. These prompts correspond to the four key components of our method: variable generation

($\mathcal{P}_{\text{var}}(X, Y, T)$ in Eq. (4)), distribution type inference ($\mathcal{P}_{\text{dist}}(X, Y, T, \hat{U})$ in Eq. (5)), parameter estimation ($\mathcal{P}_{\text{param}}(x_i, t_i, y_i)$ in Eq. (6)), and counterfactual outcome imputation ($\mathcal{P}_{\text{out}}(x_i, u_i, y_i, t_i)$ in Eq. (7)). All corresponding equations are provided in the main paper, and this appendix serves to elaborate on the concrete prompt implementations used for each component.

E.1 Prefix Prompt

The prefix prompt provides essential contextual information about the observational dataset, including a brief overview and detailed descriptions of the treatment, outcome, and confounding variables. This prompt serves as a foundation and should be included at the beginning of all subsequent prompts to ensure that the LLM is aware of the data background and variable semantics.

Prefix prompt: Dataset Introduction

Inputs: The dataset name $\mathcal{D}_{\text{name}}$ with a brief introduction $\mathcal{D}_{\text{intro}}$; variable names for confounders X_{name} , treatment T_{name} , and outcome Y_{name} ; and their corresponding descriptions as provided by the original dataset: X_{desc} , T_{desc} , and Y_{desc} .

Prompt:

Brief introduction of the $\{\mathcal{D}_{\text{name}}\}$ dataset: $\{\mathcal{D}_{\text{intro}}\}$

This observational dataset contains:

- (1) Treatment — $\{T_{\text{name}}\}$: $\{T_{\text{desc}}\}$
- (2) Outcome — $\{Y_{\text{name}}\}$: $\{Y_{\text{desc}}\}$
- (3) Confounders — $\{X_{\text{name}}\}$: $\{X_{\text{desc}}\}$

E.2 Variable Generation

In this prompt, we mainly utilize the name and description of variables X , T and Y in the observational dataset to infer a new confounder \hat{U} .

$\mathcal{P}_{\text{var}}(X, Y, T)$: Generating new confounder \hat{U}

Inputs: Prefix Prompt

Outputs: Confounder name \hat{U}_{name} , a brief explanation \hat{U}_{exp}

Prompts:

{Prefix prompt}

Based on your WORLD KNOWLEDGE, please propose one additional confounder which BOTH affects the treatment and outcome.

Make sure that the proposed confounder has a DIFFERENT MEANING compared to existing confounders.

For this proposed confounder, please provide:

- (1) A clear name for the confounder.
- (2) A brief explanation of why it affects both treatment and outcome.

E.3 Distribution type inference

After identifying the confounder variable, we leverage the commonsense knowledge embedded in LLMs to infer an appropriate distribution type for it. Instead of directly imputing its values using the LLM, which often leads to degenerate or collapsed outputs when applied to tabular data, we defer value imputation to a subsequent structured process.

$\mathcal{P}_{\text{dist}}(X, Y, T, \hat{U})$: Inferring the distribution type of \hat{U}

Inputs: Prefix prompt, name of generated variable \hat{U}_{name}

Outputs: Distribution type $\mathcal{F}_{\hat{U}}$

Prompts:

{Prefix Prompt}

Based on your WORLD KNOWLEDGE, please provide the distribution type of confounder $\{\hat{U}_{\text{name}}\}$. For example:

- (1) Continuous — e.g., Normal distribution
- (2) Discrete — e.g., Multi-categorical distribution
- (3) Binary — e.g., Bernoulli distribution

E.4 Parameter Estimation

Given the inferred distribution type $\mathcal{F}_{\hat{U}}$ of the confounder \hat{U} , the next step is to estimate the corresponding distribution parameters. As there are various possible distribution families, we illustrate the parameter estimation process using the normal distribution as an example.

$\mathcal{P}_{\text{param}}(\mathcal{D}_X, \mathcal{D}_T, \mathcal{D}_Y)$: Generating the distribution parameter for each unit

Inputs: Prefix prompt, the confounder name \hat{U}_{name} , the values of confounder \mathcal{D}_X , treatment \mathcal{D}_T and outcome \mathcal{D}_Y

Outputs: Distribution parameter $\theta_i = \{\mu_i, \sigma_i\}$ for each individual i

Prompts:

{Prefix prompt}

The values of existing confounders, treatments, and outcomes are given by:

- (1) Confounder Values: $\{\mathcal{D}_X\}$
- (2) Treatment Values: $\{\mathcal{D}_T\}$
- (3) Outcome Values: $\{\mathcal{D}_Y\}$

For the confounder $\{\hat{U}_{\text{name}}\}$, please specify a normal distribution (mean and standard deviation) for each individual from which we can sample the confounder value.

To accommodate the token limitations of LLMs, this prompt is executed in a mini-batch manner. Once the distribution parameters (e.g., mean and standard deviation in the case of a normal distribution) are obtained, we sample concrete values of the confounder \hat{U} from the personalized distribution for each instance.

E.5 Counterfactual Outcome Imputation

To evaluate the effectiveness of the generated confounders, we assess whether the unconfoundedness assumption holds after incorporating them. Since LLMs implicitly encode a wide range of commonsense and domain-specific knowledge—including information related to potential hidden confounders—we utilize the LLM to impute counterfactual outcomes, \hat{Y}^0 and \hat{Y}^1 . These counterfactuals are then used to perform an empirical test of the unconfoundedness assumption via conditional independence analysis.

$\mathcal{P}_{\text{out}}(\mathcal{D}_X, \mathcal{D}_{\hat{U}}, \mathcal{D}_T, \mathcal{D}_Y)$: Imputing Counterfactual Outcomes

Inputs: Prefix prompt, the values of confounder \mathcal{D}_X , imputed confounder $\mathcal{D}_{\hat{U}}$, treatment \mathcal{D}_T and outcome \mathcal{D}_Y

Outputs: Counterfactual outcomes in \hat{Y}^0 and \hat{Y}^1

Prompts:

{Prefix prompt}

The values of existing confounders, treatments, and outcomes are given by:

(1) Confounders: $\{\mathcal{D}_X\}$

(2) Treatments: $\{\mathcal{D}_T\}$

(3) Outcomes: $\{\mathcal{D}_Y\}$

Based on the OBSERVED DATA and your WORLD KNOWLEDGE, please infer the values of the counterfactual outcome corresponding to the alternative value of treatment.

F Case Study

In this section, we provide two running samples from Jobs dataset for both variable generation and value imputation.

F.1 Case on Variable Generation

Generating New Variable {TRANSPORTATION ACCESS}

Prompts:

Brief introduction of the {Jobs} dataset:

{The Jobs dataset is widely used in causal inference research for evaluating the performance of treatment effect estimation methods. It is constructed by combining experimental and observational data from the National Supported Work (NSW) demonstration and comparison group data (e.g., PSID or CPS).}

This observational dataset contains:

(1) Treatment — {Participation in Job Training}: $\{T \in \{0, 1\}\}$ indicating whether the individual participated or did not participate in the job training program.}

(2) Outcome — {Employment Status}: {The individual's employment observed after the treatment decision. $Y = 1$ means employed, $Y = 0$ means not employed.}

(3) Confounders — {Age, Marriage, Previous Earning,...}: {Features affecting both

the treatment and the outcome, such as age, education, prior income, etc.}

Based on your WORLD KNOWLEDGE, please propose one additional confounder which BOTH affects the treatment and outcome.

Make sure that the proposed confounder has a different meaning compared to existing confounders.

For this proposed confounder, please provide:

- (1) A clear name for the confounder.
- (2) A brief explanation of why it affects both treatment and outcome.

Answers:

- (1) Variable Name: Transportation Access
- (2) Explanation: Access to reliable transportation can influence both participation in the job training program (treatment) and subsequent employment (outcome). Individuals without transportation may be less likely to enroll in or attend the program due to logistical barriers. Similarly, lack of transportation can hinder job search efforts and commuting to workplaces, reducing the likelihood of employment.

F.2 Case on Value Imputation

Inferring Distribution Type for New Variable {TRANSPORTATION ACCESS}

Prompts:

Brief introduction of the {Jobs} dataset:

{The Jobs dataset is widely used in causal inference research for evaluating the performance of treatment effect estimation methods. It is constructed by combining experimental and observational data from the National Supported Work (NSW) demonstration and comparison group data (e.g., PSID or CPS).}

This observational dataset contains:

- (1) Treatment — {Participation in Job Training}: $\{T \in \{0, 1\}$ indicating whether the individual participated or did not participate in the job training program.}
- (2) Outcome — {Employment Status}: {The individual's employment observed after the treatment decision. $Y = 1$ means employed, $Y = 0$ means not employed.}
- (3) Confounders — {Age, Marriage, Previous Earning,...}: {Features affecting both the treatment and the outcome, such as age, education, prior income, etc.}

Based on your WORLD KNOWLEDGE, please provide the distribution type of confounder {Transportation Access}. For example:

- (1) Continuous — e.g., Normally distribution

- (2) Discrete — e.g., Multi-categorical distribution
- (3) Binary — e.g., Bernoulli distribution

Answers:

- (1) Distribution Type: Binary
- (2) Value Description: 0 indicates the individual lacks reliable transportation (e.g., no personal vehicle or inadequate public transit access), and 1 indicates they have reliable transportation.

Estimating Values for New Binary Confounder {TRANSPORTATION ACCESS}

Prompts:

Brief introduction of the {Jobs} dataset:

{The Jobs dataset is widely used in causal inference research for evaluating the performance of treatment effect estimation methods. It is constructed by combining experimental and observational data from the National Supported Work (NSW) demonstration and comparison group data (e.g., PSID or CPS).}

This observational dataset contains:

- (1) Treatment — {Participation in Job Training}: $\{T \in \{0, 1\}$ indicating whether the individual participated or did not participate in the job training program.}
- (2) Outcome — {Employment Status}: {The individual's employment observed after the treatment decision. $Y = 1$ means employed, $Y = 0$ means not employed.}
- (3) Confounders — {Age, Marriage, Previous Earning,...}: {Features affecting both the treatment and the outcome, such as age, education, prior income, etc.}

The values of existing confounders, treatments, and outcomes are given by:

- (1) Confounder Values: {[47,12,...,0], ..., [40, 8, ..., 0]}
- (2) Treatment Values: {0,0,1,0,...,1}
- (3) Outcome Values: {1,0,0,1,...,0}

For the new confounder {Transportation Access}, please specify a binary value for each individual.

Answers:

- (1) Values: [0,0,0,...,1]
- (2) Summary: The first 82 individuals (previous earning = 0) lack reliable transportation (Transportation Access = 0), while the remaining 68 (previous earning > 0) have access (Transportation Access = 1). This aligns with prior earnings as a proxy for transportation availability, creating a plausible confounder structure.

G Broader Impacts

This work introduces ProCI, a framework that uses LLMs to help mitigate hidden confounding when estimating treatment effects from observational data. By combining structured and unstructured data with the general knowledge and reasoning abilities of LLMs, ProCI offers a new and useful way to improve causal inference. In practice, the ProCI framework can improve decision-making in areas where running controlled experiments is difficult or unethical, such as healthcare, social programs, and economic policies. It can help uncover hidden confounders that affect treatment and outcomes, leading to fairer and more informed decisions—especially in places with limited resources. Also, by reducing the need for expert-designed tools or domain knowledge, ProCI makes causal analysis easier and more available to a wider group of researchers and practitioners.

H Limitations

While our proposed method consistently outperforms base models across benchmarks, it still exhibits several limitations that warrant further investigation:

- Our evaluation is conducted on two widely-used observational benchmarks—Twins and Jobs. To better assess the generalizability of the ProCI framework, future work should explore a broader range of real-world and domain-specific datasets.
- As noted in Theorem 1, the empirical unconfoundedness test using Kernel Conditional Independence Test (KCIT) on imputed counterfactuals approximates the true test only when the sample size is sufficiently large. More robust or distribution-free statistical tests may be needed to relax this assumption in smaller datasets.
- While our study extends confounder generation to include four distinct LLMs—GPT-4o, DeepSeek-R1, LLaMA 3–8B, and Qwen2.5–7B—these models primarily represent instruction-tuned decoders. Future work should further examine ProCI’s applicability across a wider range of architectures, such as multilingual models, encoder-decoder frameworks, or smaller-scale LLMs, to comprehensively assess its robustness and scalability.